Recovery of Methane from Hydrate Formed in a Variable Volume Bed of Silica Sand Particles

ARTICLE *in* ENERGY & FUELS · NOVEMBER 2009

Impact Factor: 2.79 · DOI: 10.1021/ef900543v

Energy Fuels **2009,** *23,* 5508–5516 · DOI:10.1021/ef900543v
Published on Web 09/24/2009

energy&fuels
article

Recovery of Methane from Hydrate Formed in a Variable Volume Bed of Silica Sand Particles

Praveen Linga,[†] Cef Haligva,[†] Sung Chan Nam,[‡] John A. Ripmeester,[§] and Peter Englezos*,[†]

[†]*Department of Chemical and Biological Engineering, University of British Columbia, Vancouver, BC, Canada V6T 1Z3,* [‡]*Energy Conversion Research Department, Korea Institute of Energy Research, Yuseong-gu, Daejeon, Korea 305-343, and* [§]*Steacie Institute for Molecular Sciences, National Research Council Canada, Ottawa, ON, Canada K1A 0R6*

Received May 27, 2009. Revised Manuscript Received August 31, 2009

The decomposition of methane hydrate crystals formed in sediment at 1.0, 4.0, and 7.0 °C was studied in a new apparatus designed to accommodate three different size volume beds of silica sand particles. The sand particles are microporous with a 0.9 nm pore diameter and have an average diameter equal to 329 μm. The hydrate was formed in the interstitial spaces between sand particles, and the hydrate crystal decomposition was driven by heating (thermal stimulation). The amount of methane released from the dissociating hydrate in each experiment (methane recovery curve) was determined, and it was shown that the release of gas proceeds in two stages in terms of rate. The rate of methane release (recovery) per mole of water depends on the bed size for the first stage of hydrate dissociation. The second stage rate does not depend on the bed size. This work suggests that the comparison of simulated data to experimental results from laboratory synthesized hydrate and possibly from natural samples should be done with more than one sample-size data.

1. Introduction

Methane and other natural gas components are found stored in the earth in a crystalline form known as gas or clathrate hydrate.[1] The first indication of naturally occurring gas hydrates outside of the Soviet Union was the report by Stoll et al.[2] On the basis of wireline logs from two exploratory wells in the Mackenzie Delta, Canada, Bily and Dick[3] concluded that gas hydrates were contained in shallow sand reservoirs. As soon as the significance of the natural gas potential of gas hydrates stored in the earth was realized, efforts to develop extraction methods started.[4−9] Potential reserves of natural gas hydrates are over 1.5×10^{16} m^3 and are distributed all over the earth on land in the Arctic and offshore.[10−13] Gas hydrates are nonstoichiometic, crystalline, inclusion compounds.[14,15] For about eight decades they have been known to plug hydrocarbon pipelines.[16]

Two reports from the Los Alamos National laboratory presented the first state of the art analysis and pointed out the difficulties associated with natural gas recovery techniques.[7,17,18] Holder et al.[19] concluded that reservoir porosity and the thermal properties of the hydrates and the reservoir were limiting factors that would determine whether a gas hydrate reservoir could produce gas in an energy efficient manner. It was also realized during these early studies that knowledge of the rate of hydrate decomposition is required. A reliable assessment of the feasibility of producing natural gas from the earth's naturally occurring hydrates requires several pieces of key information.[20] Although some are reservoir-specific, others such as dissociation kinetics have general applicability and can be evaluated in the laboratory.[20] Although significant progress has been made regarding modeling and numerical simulation

*To whom correspondence should be addressed. Telephone: 1-604-822-6184. Fax: 1-604-822-6003. E-mail: englezos@interchange.ubc.ca.

(1) Makogon, Y. F.; Trebin, F. A.; Trofimuk, A. A.; Tsarev, V. P.; Cherskii, N. *Doklady Akademii Nauk SSSR* **1971**, *196*, 203–206.
(2) Stoll, R. D.; Ewing, J.; Bryan, G. M. *J. Geophys. Res.* **1971**, *76* (8), 2090–2094.
(3) Bily, C.; Dick, J. W. L. *Bull. Can. Pet. Geol.* **1974**, *22* (3), 340–352.
(4) Davidson, D. W.; El-Defrawy, M. K.; Fuglem, M. O.; Judge, A. S. *Int. Conf. Permafrost Proc.* **1978**, *3* (1), 937–943.
(5) Bowsher, A. L. Proceedings of a Workshop on Clathrates in NPRA held in Menlo Park 7/16−17/79 USGS Open File Report *81−1298*; 1981; pp 0−164.
(6) Stoll, R. D.; Bryan, G. M. *J. Geophys Res.* **1979**, *84* (B4), 1629.
(7) Barraclough, B. L. Methane Hydrate Resource Assessment Program. *Los Alamos Sci Lab Progr Rep No. LA-8569-PR*; April−June 1980; p 27.
(8) Makogon, Y. F. *Perspectives for the Development of Gas-Hydrate Deposits*; 4th Can. Permafrost Conf. Proc., R.J.E. Brown Memor. Vol.; 1982; pp 299−304.
(9) Judge, A. *Natural Gas Hydrates in Canada*; 4th Can. Permafrost Conf. Proc., R.J.E. Brown Memor. Vol.; 1982; pp 320−328.
(10) Kvenvolden, K. *Proc. Natl. Acad. Sci. US* **1999**, *96*, 3420.
(11) Milkov, A. V.; Dickens, G. R.; Claypool, G. E.; Lee, Y. J.; Borowski, W. S.; Torres, M. E.; Xu, W. Y.; Tomaru, H.; Trehu, A. M.; Schultheiss, P. *Earth Planetary Sci.Lett.* **2004**, *222* (3−4), 829–843.
(12) Kvenvolden, K. A. *Rev. Geophys.* **1993**, *31* (2), 173–187.
(13) Makogon, Y. F.; Holditch, S. A.; Makogon, T. Y. *J. Pet. Sci. Eng.* **2007**, *56* (1−3), 14–31.
(14) Davidson, D. W., *Gas Hydrates. In Water: A Comprehensive Treatise*; Plenum Press: New York, 1973; Vol. 2, p 115−234.
(15) Sloan, E. D., Jr., *Clathrate Hydrates of Natural Gases*, Second ed., Revised and Expanded. Marcel Dekker: New York, 1998; p 754.
(16) Hammerschmidt, E. G. *Ind. Eng. Chem.* **1934**, *26* (8), 851–855.
(17) McGuire, P. L. Methane Hydrate Gas Production: An Assessment of Conventional Production Technology as Applied to Hydrate Recovery. *LASL Report LA-9102-MS, Order No. DE82006746 from NTIS*; 1981; p 20.
(18) McGuire, P. L. *Methane Hydrate Gas Production by Thermal Stimulation*; 4th Can. Permafrost Conf, Calgary 3/2−6/81, R.E. Brown Memor. Vol.; 1982; p 356−362.
(19) Holder, G. D.; Angert, P. F.; John, V. T.; Yen, S. A. *J. Petrol Tech.* **1982**, *34* (5), 1127–1132.
(20) Kneafsey, T. J.; Tomutsa, L.; Moridis, G. J.; Seol, Y.; Freifeld, B. M.; Taylor, C. E.; Gupta, A. *J. Pet. Sci. Eng.* **2007**, *56* (1−3), 108–126.

of natural gas hydrate reservoirs,[21−27] few papers in the literature present experimental data on hydrate formation and decomposition kinetics investigated in porous media.[20,28−38] Selim and Sloan[37] used thermal stimulation to decompose hydrates formed in porous media in the laboratory. The dissociation rate was found to depend on the thermal properties and the porosity of the reservoir. Further work that was reported from Sloan's laboratory found that endothermic hydrate decomposition processes could cause such a temperature drop that hydrates might reform or water could freeze.[39,40] Handa and Stupin[28] reported thermodynamic properties and dissociation characteristics of methane and propane in silica gel pores. Stern et al.[29] observed the peculiarities of methane clathrate hydrate formation and solid state deformation. However the observations[28,29] were made at < 105 K and 10^{-3} Pa, whereas in the natural environment such samples have pressures approximately 3 to 10 MPa and above-freezing temperatures.[20] The complexity of hydrate dissociation was also highlighted by Tsimpanogiannis and Lichtner[41] who also presented a thorough literature review along with a parametric study of methane hydrate dissociation in oceanic sediments driven by thermal stimulation.

Kneafsey et al.[20] studied methane hydrate formation in a bed of silica sand using an X-ray transparent pressure vessel. They highlighted the need for multiple means of measurement, which is critical for understanding hydrate behavior during hydrate formation/decomposition. They also reported that the rate of hydrate formation is not always proportional to the driving force, that is, might increase as the pressure is reduced toward the equilibrium value. They attribute this counterintuitive result to the exsolution of methane in the water. Tang et al.[32] studied the production behavior of gas hydrate under thermal stimulation in unconsolidated sediment. They reported that the gas production rate increased with time until it reached a maximum and then it began to decrease. Kono et al.[35] reported that the decomposition rates can be adjusted by controlling the sediment properties. They formed methane hydrate in various custom-designed porous sediments (glass beads) at experimental conditions of 273.5 K and pressures between 6.8 and 13.6 MPa.[35] Recently, Liu et al.[33] reported through Raman studies on methane hydrate decomposition in sand that the change in the intensity ratio of large to small cages were consistent with respect to bulk hydrate but dropped dramatically after some time, and this turning point was found to be related to particle size of the sand. This behavior was observed for sands with particle size below 106 μm. The particle sizes of the sands were 53−75, 90−106, 106−150, and 150−180 μm.[33]

One of the aspects that was not examined in previous laboratory studies with synthetic hydrate samples or samples recovered from the earth is the impact of the sample size on the rate with which the gas is released from the sample during thermal stimulation or depressurization. It should be noted, however, that Handa[42] briefly discussed the sample size of a naturally occurring hydrate in the context of calorimetric measurements. Such information is useful if the collected data are to be used to test the validity of numerical simulation schemes for hydrate dissociation. Thus, the objective of this work is to study the kinetics of hydrate decomposition in a new apparatus that was specifically designed to investigate the potential dependency of the results on the size of the silica sand bed. The gas recovery rate during decomposition, along with the temperature profiles at various locations in the bed, is presented. The kinetics study of hydrate formation in the same apparatus is presented separately.[43]

2. Experimental Section

UHP grade methane (Praxair Technology Inc.) and distilled and deionized water was used. The diameter of the silica sand particles ranged from 150 to 630 μm and had an average value of 329 μm. The sand particles were supplied by Sigma-Aldrich (catalog number: 274739). The BET surface area of the sand was found to be 0.3499 cm^2/g and that the sand has micropores with a pore volume of 0.000 152 cm^3/g and an average pore diameter of 0.90 nm. The pore volume and pore diameter were calculated using the Horvath−Kawazoe method.[44]

2.1. Apparatus. Figure 1 shows the schematic of the apparatus. It consists of a crystallizer (CR) that is a cylindrical vessel (I.D. = 10.16 cm, height = 15.24 cm). The gas released during decomposition is collected in a reservoir (R). The crystallizer and the reservoir are immersed in a temperature-controlled water bath. Pressure is measured with Rosemount smart pressure transmitters (model 3051, Norpac controls, Vancouver, BC). The maximum uncertainty is 0.075% of the span (0−15 000 kPa), that is, 11 kPa. The temperatures of the hydrate phase and the gas phase of the crystallizer are measured using Omega copper-constantan thermocouples with an uncertainty of 0.1 K.

(21) Moridis, G.; Collett, T. S.; Dallimore, S. R.; Satoh, T.; Hancock, S.; Weatherill, B. In *Numerical Simulation Studies of Gas Production Scenarios From Hydrate Accumulations at the Mallik Site, Mackenzie Delta, Canada*, Proc. 4th International Conference on Gas Hydrates, Yokohama, May 19−23, 2002; Yokohama, 2002; pp 239−244.
(22) Moridis, G. J. *SPE J.* **2003**, *8* (4), 359–370.
(23) Moridis, G. J. *SPE Reservoir Eval. Eng.* **2004**, *7* (3), 175–183.
(24) Moridis, G. J.; Collett, T. S.; Dallimore, S. R.; Satoh, T.; Hancock, S.; Weatherill, B. *J. Pet. Sci. Eng.* **2004**, *43* (3−4), 219–238.
(25) Moridis, G. J.; Kowalsky, M. B. *SPE J.* **2007**, *12* (2), 253–268.
(26) Kowalsky, M. B.; Moridis, G. J. *Energy Convers. Manage.* **2007**, *48* (6), 1850–1863.
(27) Gerami, S.; Pooladi-Darvish, M. *J. Pet. Sci. Eng.* **2007**, *56* (1−3), 146–164.
(28) Handa, Y. P.; Stupin, D. *J. Phys. Chem.* **1992**, *96*, 8599.
(29) Stern, L. A.; Kirby, S. H.; Curham, W. B. *Science* **1996**, *273* (5283), 1843–1848.
(30) Sakamoto, Y.; Komai, T.; Kawamura, T.; Minagawa, H.; Tenma, N.; Yamaguchi, T. *Int. J. Offshore Polar Eng.* **2007**, *17* (1), 47–56.
(31) Katsuki, D.; Ohmura, R.; Ebinuma, T.; Narita, H. *Philos. Mag.* **2007**, *87* (7), 1057–1069.
(32) Tang, L. G.; Xiao, R.; Huang, C.; Feng, Z. P.; Fan, S. S. *Energy Fuels* **2005**, *19* (6), 2402–2407.
(33) Liu, C. L.; Lu, H. L.; Ye, Y. G.; Ripmeester, J. A.; Zhang, X. H. *Energy Fuels* **2008**, *22* (6), 3986–3988.
(34) Sung, W. M.; Lee, H.; Kim, S.; Kang, H. *Energy Sources* **2003**, *25* (8), 845–856.
(35) Kono, H. O.; Narasimhan, S.; Song, F.; Smith, D. H. *Powder Technol.* **2002**, *122* (2−3), 239–246.
(36) Sun, C. Y.; Chen, G. J. *Fluid Phase Equilib.* **2006**, *242* (2), 123–128.
(37) Selim, M. S.; Sloan, E. D. *Soc. Petr. Eng. Reservoir Eng.* **1990**, 245.
(38) Kamata, Y.; Ebinuma, T.; Omura, R.; Minagawa, H.; Narita, H.; Masuda, Y.; Konno, Y. In *Decomposition Experiment of Methane Hydrate Sediment by Thermal Recovery Method*, 5th International conference on gas hydrates, Trondheim, June 12−16, 2005; Trondheim, 2005.
(39) Yousif, M. H.; Abass, H. H.; Selim, M. S.; Sloan, E. D. *SPE Reservoir Eng.* **1991**, *6* (1), 69–76.
(40) Yousif, M. H.; Sloan, E. D. *SPE Reservoir Eng.* **1991**, *6* (4), 452–458.
(41) Tsimpanogiannis, I. N.; Lichtner, P. C. *J. Pet. Sci. Eng.* **2007**, *56* (1−3), 165–175.
(42) Handa, Y. P. *Ind. Eng. Chem. Res.* **1988**, *27* (5), 872–874.
(43) Linga, P.; Haligva, C.; Nam, S. C.; Ripmeester, J. A.; Englezos, P. *Energy Fuels* **2009**, DOI: 10.1021/ef900542m.
(44) Horvath, G.; Kawazoe, K. *J. Chem. Eng. Jpn.* **1983**, *16* (6), 470–475.

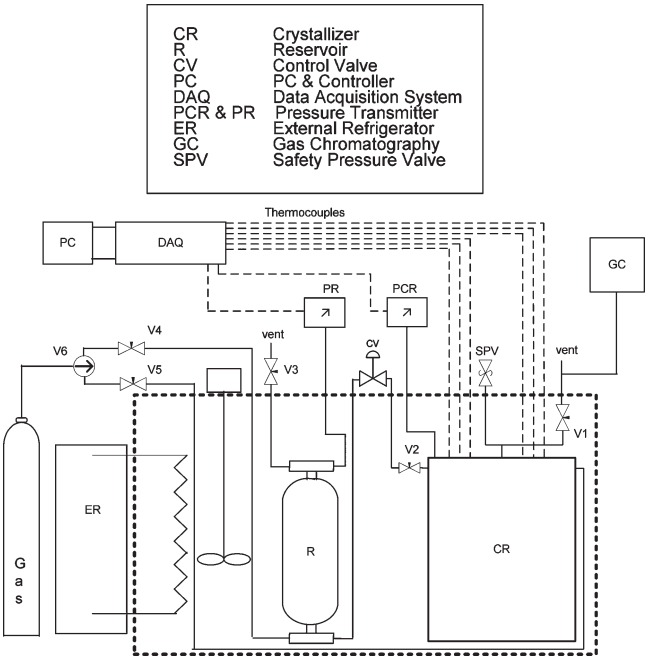

Figure 1. Apparatus.

Seven thermocouples are located in the crystallizer with one in the gas phase and six in the silica sand bed. Constant pressure during decomposition is obtained by a PID controller and a control valve (Fisher Bauman). The data acquisition system (National Instruments) is coupled with a computer to record the data as well as to communicate with the control valve during the experiment. The software used for this purpose is LabView 8.0 (National Instruments). The apparatus is also equipped with a safety pressure valve.

Figure 2a, shows the location of the seven thermocouples in the crystallizer. In order to study the effect of the variable volume of the silica sand bed on hydrate formation and decomposition, two copper cylinders are placed inside the crystallizer as shown in Figure 2b. The reason we chose copper cylinders to place in the hydrate vessel and decrease the sample size is because heat transfer resistance through copper (copper thermal conductivity = 400 W/mK[45]) is minimized. The first copper cylinder (CC_1) has a diameter of 7.62 cm (3 in) and the second one (CC_2) is 5.08 cm (2 in). The wall thickness of both cylinders is 1.27 cm (0.5 in). Both copper cylinders fit precisely in the crystallizer. The placement of the copper cylinders is seen in Figure 3. It is noted that only four thermocouples could be accommodated in the silica bed with both CC_1 and CC_2 present in the crystallizer (Figure 2b).

2.2. Procedure. *2.2.1. Formation Experiment*. The procedure for the formation experiment is described in detail in the formation paper.[43] Briefly, a 7.0 cm (height) bed of silica sand is created by placing 914.1 g of sand in the crystallizer. The volume of water required to fill the void space with water (100% saturation) was found to be 0.217 cm^3/g which is the interstitial or pore volume of the bed of sand particles. Accordingly, 198.5 mL of water was added to the sand. The amount of the sand placed in the crystallizer was reduced to 513.7 g and 228.5 g when one (CC_1) or two (CC_1+CC_2) copper cylinders are present, respectively. The height of the silica sand bed remained the same (7.0 cm). The bed was prepared by splitting the required amount of sand and water into five equal parts and placing each in a batch order (sand + water) to form a uniform bed and also to eliminate the presence of any pockets of air in the bed. Subsequently, the crystallizer is pressurized with methane to 2.5 MPa and depressurized to atmospheric pressure three times. The pressure in the crystallizer is then set to the desired value. When the temperature reaches the target temperature (approximately 5 min) then the data is logged. All hydrate formation experiments are carried out with a fixed amount of water and gas. The temperature in the crystallizer was maintained constant by providing cooling externally. When hydrate formation occurs, gas will be consumed and hence the pressure in the closed system drops. Typically, the experiment was allowed to continue until there is no significant change in the rate of pressure drop in the crystallizer. Finally, the pressure and temperature data are used to calculate the moles of methane consumed in the crystallizer (gas uptake). This is equal to the number of moles in the gas phase of the crystallizer and the tubing at time zero minus the number of moles at the end of the experiment.[43,46]

2.2.2. Decomposition Experiment. After the completion of each hydrate formation experiment, the hydrates were decomposed at a constant pressure as follows. The pressure in the crystallizer was decreased to the desired pressure (20% above the equilibrium hydrate formation pressure). The temperature in the crystallizer was then allowed to become stable (to reach 4.0 °C, if the formation experiment was conducted at 4.0 °C). This takes less than about 10 min. The temperature of the crystallizer was then increased to the desired value by heating the water bath with an external refrigerator/heater. This is time zero for the decomposition experiment, and the data is recorded. Note that during this step there was no decomposition taking place since the temperature in the crystallizer was below the equilibrium temperature at the experimental pressure. For example, the decomposition temperature for methane hydrate at 4.6 MPa is 5.7 °C. During the experiment, when the temperature of the crystallizer crosses the equilibrium phase boundary, the hydrate starts to decompose, and since the pressure in the crystallizer was maintained constant by the PID controller, the excess gas was released from the crystallizer and collected in the reservoir (R). The experiment proceeded until there was no further release of methane gas from the hydrate.

At any given time, the total number of moles ($n_{T,t}$) in the system remains constant and equal to that at time zero ($n_{T,0}$). The system in this case includes the crystallizer (CR), the reservoir (R), and the connecting tubing. During the decomposition experiment the pressure in the crystallizer is kept constant. Hence, the gas released from the hydrate during the experiment is collected in the reservoir (R). A PID controller coupled with a control value is employed for this purpose. The total number of moles at any given time is the sum of the number of moles (n_G) in gas phase (G) of the crystallizer, the number of moles (n_R) collected in the reservoir, and the number of moles (n_H) in the hydrate phase. The number of moles of gas released from the hydrate at any time during hydrate decomposition can then be calculated as follows,

$$n_{H,0} - n_{H,t} = n_{G,t} - n_{G,0} + n_{R,t} - n_{R,0} \quad (1)$$

or

$$\Delta n_{H,\uparrow} = n_{H,0} - n_{H,t} = \left(\frac{PV}{zRT}\right)_{G,t} - \left(\frac{PV}{zRT}\right)_{G,0} + \left(\frac{PV}{zRT}\right)_{R,t} - \left(\frac{PV}{zRT}\right)_{R,0} \quad (2)$$

where z is the compressibility factor calculated by Pitzer's correlation.[47]

(45) Incropera, F. P.; DeWitt, D. P., *Fundamentals of Heat and Mass Transfer*, Fifth ed.; John Wiley & Sons Inc.: 2002.

(46) Haligva, C. *Natural Gas Recovery from Hydrates in a Silica Sand Matrix*; University of British Columbia: Vancouver, 2008.

(47) Smith, J. M.; Van Ness, H. C.; Abbott, M. M., *Introduction to Chemical Engineering Thermodynamics*; McGraw-Hill, Inc.: New York, 2001.

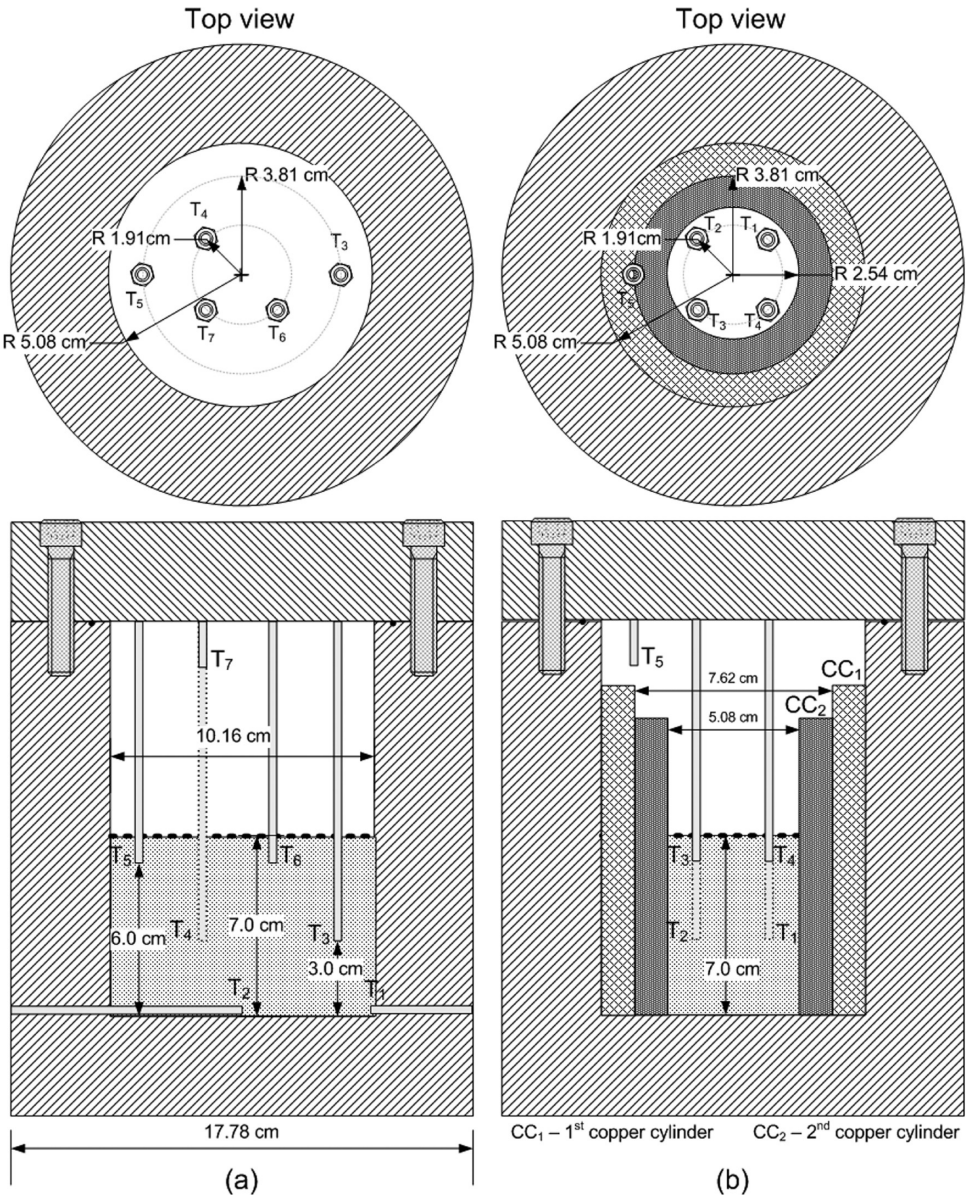

Figure 2. Cross section and top view of the crystallizer showing, (a) location of the thermocouples with in the crystallizer without the copper cylinders (b) arrangement of the copper cylinders (CC_1 and CC_2) in the crystallizer, and the location of the thermocouples.

The percent methane recovery is calculated as a function of time for any given decomposition experiment based on information obtained from its formation experiment and is calculated by the following equation:

$$\%\ \text{methane recovery} = \frac{(\Delta n_{H,\uparrow})_t}{(\Delta n_{H,\downarrow})_{t_{end}}} \times 100 \qquad (3)$$

where $(\Delta n_{H,\downarrow})_{t_{end}}$ is the number of moles consumed for hydrate formation at the end of a typical formation experiment and $(\Delta n_{H,\uparrow})_t$ is the number of moles released from hydrates during hydrate decomposition at any given time. It should be noted here that if one has a natural sample (hydrate core), then during a decomposition experiment the number of moles released $(\Delta n_{H,\uparrow})_t$ can be determined but the quantity $(\Delta n_{H,\downarrow})_{t_{end}}$ is not known.

3. Results and Discussion

Table 1 summarizes the hydrate formation experimental conditions, the amount of methane consumed to form hydrate and the water conversion to hydrate crystals. The duration of each experiment is reported in Table 1. The water conversion was calculated based on a hydration number of 6.1.[48] All experiments with the reduced size beds (CC_1 and CC_1+CC_2) were conducted at a temperature of 4.0 °C to ensure that a significant amount of hydrate exists in the bed. The decomposition experiments are summarized in Table 2. Figures 4 and 5 show the typical gas recovery curves, $(\Delta n_{H,\uparrow})_t$, obtained during Experiments 5 and 6 respectively. As seen in the figures, when the temperature exceeds 5.7 °C (equilibrium temperature at P_{exp}), hydrate starts to decompose. The pressure in the crystallizer is maintained constant, and the released gas is collected in the reservoir. When the temperature exceeds 5.7 °C, the temperature profiles are different because the temperatures depend on the heat absorbed for hydrate dissociation (hydrate dissociation is an endothermic process) and heat supplied (heat is supplied to the crystallizer by heating the

(48) Tulk, C. A.; Ripmeester, J. A.; Klug, D. D. *Gas Hydrates: Challenges Future* **2000**, *912*, 859–872.

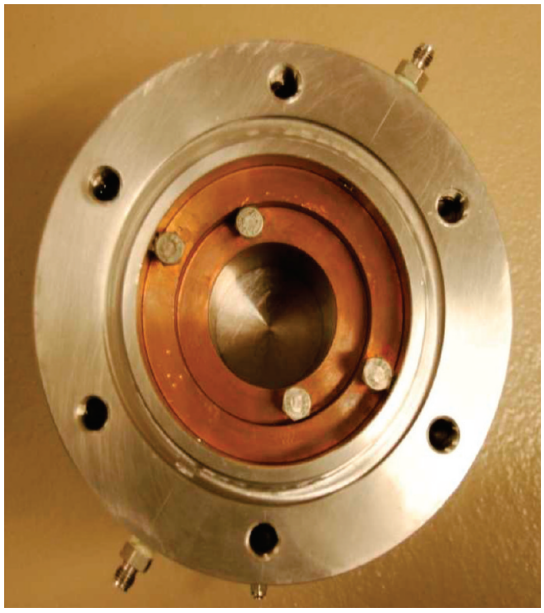

Figure 3. Arrangement of copper cylinders inside the crystallizer.

Table 1. Hydrate Formation Experimental Conditions[a]

		end of experiment		
exp. No.	T_{exp} [C]	time [hr]	CH_4 consumed [mol/mol of H_20]	water conversion to hydrate [mol %]
		CH_4/Silica Sand/Water [CR]		
1	7.0	92.5	0.0172	10.2
2	7.0	100.6	0.0180	11.0
3	4.0	71.6	0.1287	78.5
4	4.0	48.6	0.1261	77.0
5	4.0	29.0	0.1266	77.2
6	4.0	29.0	0.1215	74.1
7	1.0	65.3	0.1308	79.8
8	1.0	95.4	0.1350	82.4
		CH_4/Silica Sand/Water [CR + CC_1]		
9	4.0	61.2	0.1288	78.5
10	4.0	24.0	0.1244	75.9
11	4.0	24.0	0.1315	80.2
12	4.0	40.0	0.1381	84.3
		CH_4/Silica Sand/Water [CR + CC_1 + CC_2]		
13	4.0	46.9	0.1261	76.9
14	4.0	41.7	0.1410	85.9
15	4.0	46.7	0.1238	75.5
16	4.0	34.7	0.1603	97.8

[a] The initial pressure for all the experiments was 8.0 MPa.

bath by an external heater). The balance of these heat transfers determines the thermocouple responses. The decomposition temperatures at which methane release occurred for the other experiments carried out at 6.2 and 3.5 MPa are also given in Table 2. All the decomposition temperatures were compared with those calculated based on widely known computational method and software.[15] They were found to be in excellent agreement, as seen in Figure 6.

Figure 7 shows the temperature profiles and methane release curves for two experiments obtained with beds CC_1 (experiment 10) and CC_1+CC_2 (experiment 14) in the crystallizer for a thermal driving force of 4.0 °C. As seen by comparing the temperature profiles for the full size (CR) bed (Figure 4) with one copper (CR+CC_1) cylinder (Figure 7, top) and two copper (CR+CC_1+CC_2) cylinders (Figure 7, bottom), the temperature profiles are no longer distinct when we narrow the bed size. For example, T_6 (see Figure 2a for its position) in Figure 4 stays constant at about ~5.7 C for ~4.5 h and gradually catches up with the other thermocouples as methane release slows down. Whereas in Figure 7 (top), T_4 (as seen in Figure 2b it is located in the same position as T_6 in the full size bed) stays constant at about ~5.7 C for ~2 h when one copper cylinder is present, and in Figure 7 (bottom) T_4 follows the path of the other thermocouples. This is probably due to the heat transfer between the copper cylinder and the reactor wall (Figure 2b) being faster as compared to the heat transfer between the sand/hydrate matrix and the reactor wall (Figure 2a). The same behavior can be seen in the thermocouple readings in the decomposition experiments conducted at a higher driving force (10 °C) for the three bed sizes (Figures 5, 8-top and 8-bottom).

Figure 9 shows the methane recovery curve for Experiment 9 carried out at 4.6 MPa and a driving force ($\triangle T$) of 4.0 °C. Time zero in the figure is the time when methane release from the hydrate begins. As seen in the figure, methane recovery occurred at two stages (stages 1 and 2). Two such stages were observed for all the decomposition experiments with all bed sizes. The rate of methane release for each stage was calculated by fitting the data to a straight line. The rates are given in Table 2. As seen in Figure 9, 0.5 mols of methane are recovered in the first stage. Considering that the total amount of methane recovered from hydrate for this experiment (Experiment 9) is 0.77 mols, this corresponds to 65% recovery in the first stage. The explanation why the decomposition slows down after stage 1 can be obtained by examining Figure 4. As seen in Figure 4, around 0.79 mols are recovered in the first stage, which lasts approximately 4 h. At this time the temperatures of thermocouples T_3 and T_4 begin to increase while, T_5 and T_6 are still in the plateau indicating decomposition taking place in the region where T_5 and T_6 are located, while the decomposition appears to be completed in the region around thermocouples T_3 and T_4. Hence, during the first stage the decomposition appears to occur in the entire sample (activity detected by all thermocouples in the bed), whereas in the second stage the decomposition appears to be complete in some regions while occurring in some regions (stranded pockets), leading to a reduction in the rate of gas release.

The moles of methane released due to hydrate decomposition for the set of experiments carried out in the presence of copper cylinder CC_1 and both CC_1 and CC_2 are shown in Figures 10 (top) and 11 (top). The percent recovery of methane as a function of time was calculated using eq 3. The values are shown in Figures 10 (bottom) and 11 (bottom). As expected, the recovery of methane from hydrates was faster for the higher driving force of 10.0 °C for both cases. Complete recovery was achieved in just over 3.3 h (Figure 10 & 11) for the higher driving force, whereas it took around 12.5 h (Figure 10) for the experiments carried out at a driving force of 4.0 °C with the presence of CC_1 and around 8.3 h (Figure 11) with the presence of both CC_1 and CC_2 at the driving force of 4.0 °C. Moreover, the release curves at the same driving force are similar. The final percent recovery of methane from hydrate for the decomposition experiments are presented in Table 2. As can be seen, a percentage recovery in the range of 95−99% was obtained for all the decomposition experiments performed at 6.2, 4.6, and 3.5 MPa, respectively. It is also noted that the experimental error associated with the mole consumption calculation for each formation and

Table 2. Summary of Hydrate Decomposition Experiments along with the Rate of Recovery and Final Percent of Methane Recovered

		$\triangle T = T_{end} - T_{start}$			rate of methane release [b] [mol/h]		
exp. No	P_{exp} [MPa]	T_{start} [C]	$\triangle T$ [C]	T_d at P_{exp} [a] [C]	stage 1 (R^2 values)	stage 2 (R^2 values)	methane recovery [mol %]
				CH_4/Silica Sand/Water [CR]			
1	6.2	7.0	3.0	8.8	0.0407 (0.9981)	0.0168 (0.9345)	96.0
2	6.2	7.0	3.0	8.8	0.0524 (0.9912)	0.0123 (0.9293)	96.0
3	4.6	4.0	3.8	5.8	0.1546 (0.9939)	0.0510 (0.9944)	96.5
4	4.6	4.0	4.8	5.7	0.3020 (0.9936)	0.0921 (0.9895)	97.6
5	4.6	4.0	4.0	5.7	0.2057 (0.9886)	0.0614 (0.9833)	99.1
6	4.6	4.0	10.0	5.8	0.5306 (0.9956)	0.2379 (0.9971)	97.7
7	3.5	1.0	4.0	2.9	0.1521 (0.9855)	0.0359 (0.9826)	96.8
8	3.5	1.0	4.0	2.9	0.1400 (0.9924)	0.0316 (0.9845)	98.1
				CH_4/Silica Sand/Water [CR + CC_1]			
9	4.6	4.0	4.0	5.7	0.1371 (0.9949)	0.0324 (0.9921)	97.4
10	4.6	4.0	4.0	5.7	0.1309 (0.9926)	0.0344 (0.9960)	99.0
11	4.6	4.0	10.0	5.8	0.3374 (0.9954)	0.1330 (0.9944)	98.5
12	4.6	4.0	10.0	5.7	0.3611 (0.9954)	0.1286 (0.9947)	98.9
				CH_4/Silica Sand/Water [CR + CC_1 + CC_2]			
13	4.6	4.0	4.0	5.7	0.0827 (0.9958)	0.0180 (0.9941)	96.2
14	4.6	4.0	4.0	5.7	0.0836 (0.9947)	0.0200 (0.9957)	94.7
15	4.6	4.0	10.0	5.7	0.2137 (0.9946)	0.0645 (0.9850)	96.1
16	4.6	4.0	10.0	5.7	0.2549 (0.9947)	0.0785 (0.9957)	95.0

[a] T_d is the decomposition temperature at which methane release occurs from the hydrate for the experimental pressure, P_{exp}. [b] Rate of methane release was calculated for the two stages as shown in Figure 9.

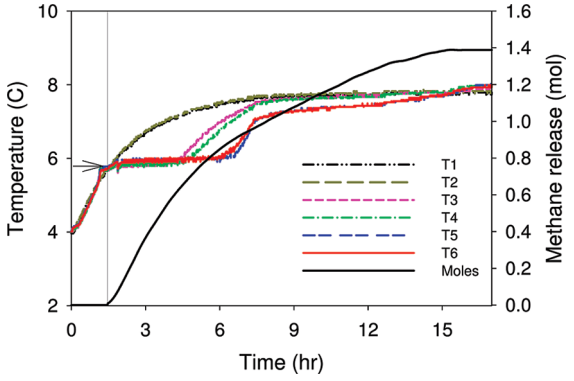

Figure 4. Typical gas recovery curve with temperature profiles for an experiment conducted in CR and at a driving force of 4.0 °C (Experiment 5, Table 2).

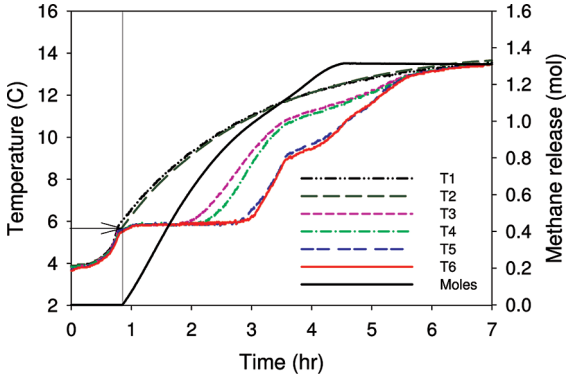

Figure 5. Typical gas recovery curve with temperature profiles for an experiment conducted in CR and at a driving force of 10.0 °C (Experiment 6, Table 2).

decomposition experiment is ±1%. The experimental error was calculated based on the error associated with the pressure transmitter and the thermocouple.[46] Also, the decomposition experiments were carried out at a certain pressure (6.2, 4.6, and 3.5 MPa, respectively) which means that a small amount (calculated at 8.8 °C and 6.2 MPa to be 1.4% of the consumed methane for hydrate formation) of methane gas that dissolved during the formation experiment remains in the liquid water and is not recoverable. This probably explains the fact that the percent recovery for all the experiments was in the range of 95−99%.

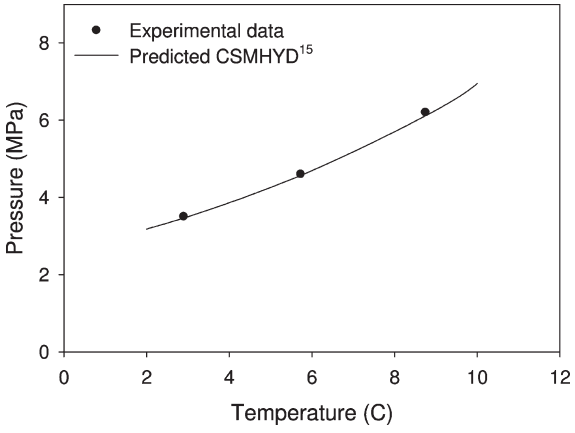

Figure 6. Comparison of decomposition temperature found by thermal stimulation for CH_4/water system in the presence of silica sand and the calculated equilibrium temperatures for CH_4/bulk water system using CSMHYD.[15]

Figure 12 shows a comparison of the percent methane recovery curves for all the decomposition experiments carried out at a constant pressure of 4.6 MPa and with a temperature driving force (ΔT) of 4.0 °C and with all the three cases; one with silica bed at its largest size (Experiment 5), one with silica bed with CC_1 inside the crystallizer (Experiments 9 and 10), and one silica bed with both CC_1 and CC_2 placed in the crystallizer (Experiments 13 and 14). As seen from the figure, the qualitative nature of the release curve is preserved as we narrow down the bed size by installing copper cylinders inside the crystallizer. Although quantitatively the curves are not identical, the final percent recoveries are approximately the same. Similar observations can be made for the

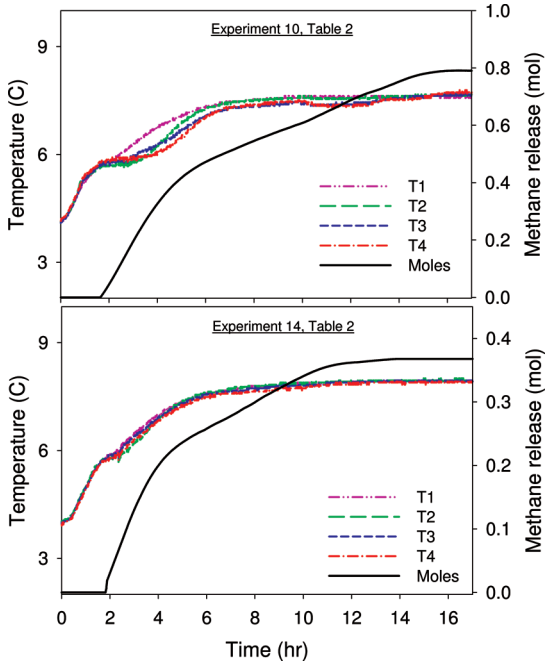

Figure 7. Gas recovery curve with temperature profiles for the experiment conducted with one copper cylinder (Experiment 10) and two copper cylinders in CR (Experiment 14) and a driving force of 4.0 °C.

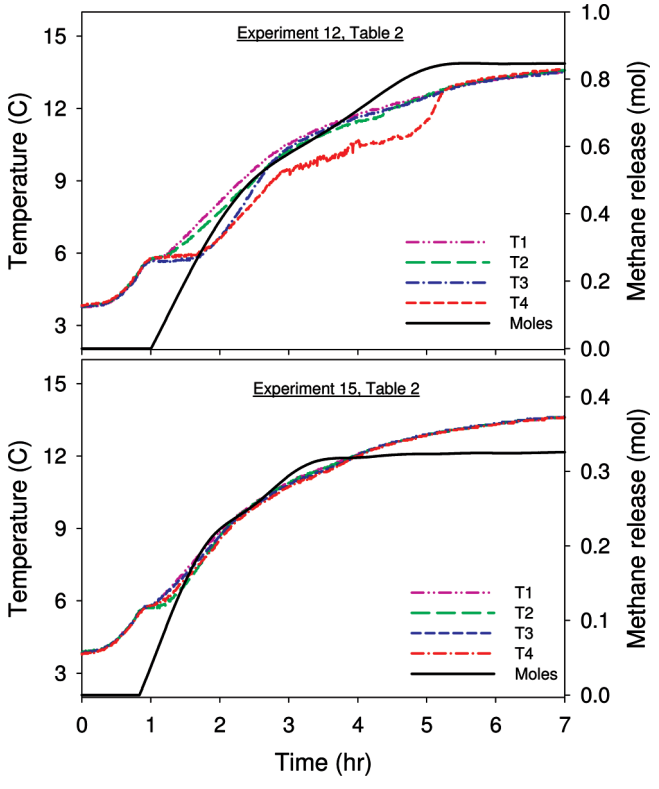

Figure 8. Gas recovery curve with temperature profiles for the experiment conducted with one copper cylinder (Experiment 12) and two copper cylinders in CR (Experiment 15) and a driving force of 10.0 °C.

results with a temperature driving force of 10.0 °C shown Figure 13.

The quantitative differences between the results with different size sand beds are better illustrated when the calculated

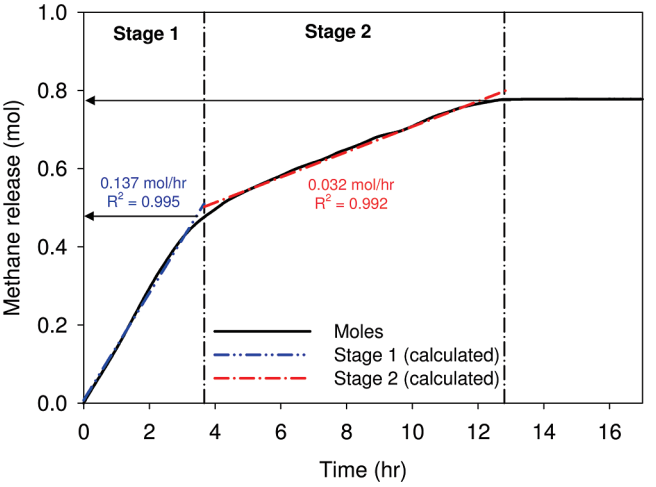

Figure 9. Methane release measurement curve from hydrate showing two stages of recovery and the calculated rate of recovery (Experiment 9, Table 2).

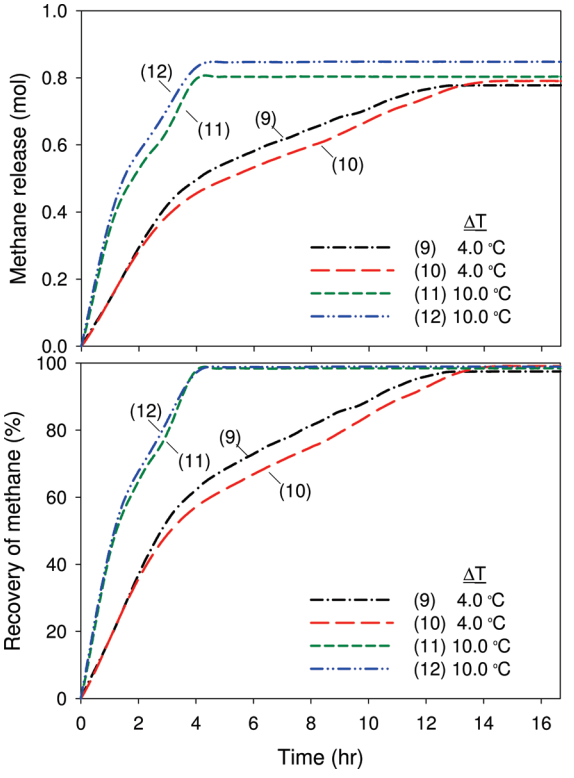

Figure 10. Moles of methane released and corresponding percent methane recovery from hydrate from the decomposition experiments carried out with the presence of CC_1 at 4.6 MPa and driving force (ΔT) of 4.0 and 10 °C. Number in the parentheses indicates the experiment number in Table 2.

rates of methane release (given in Table 2) are plotted. More specifically, the rates per mol of water are determined since the beds hold different amounts of water available for hydrate formation. Figure 14 shows the calculated rates along with the standard errors plotted against the volume of the bed for the temperature driving force of 4.0 and 10.0 °C, respectively. There is a decreasing trend in the calculated rate of methane release for the first stage as we increase the bed size while the rates are more or less the same for the second stage. Clearly, there is a strong dependency of methane recovery rate on the

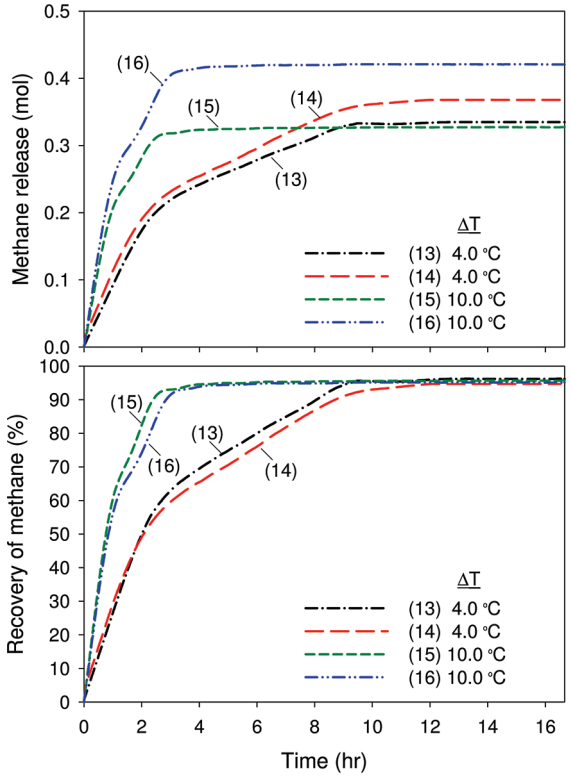

Figure 11. Moles of methane released and corresponding percent methane recovery from hydrates from the decomposition experiments carried out with the presence of CC_1 and CC_2 at 4.6 MPa and driving force ($\triangle T$) of 4.0 and 10 °C, respectively. Number in the parentheses indicates the experiment number in Table 2.

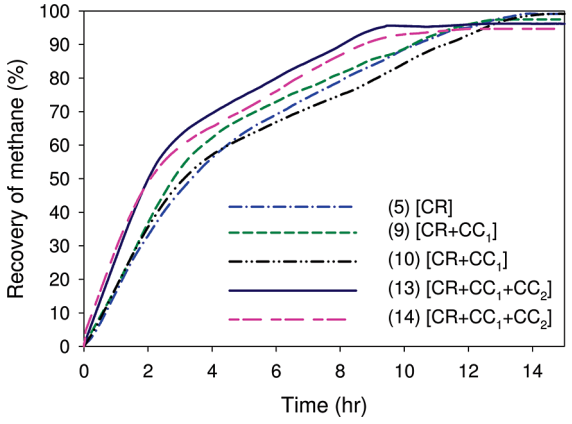

Figure 12. Comparison of methane recovery from decomposition experiments for the three different silica bed sizes studied at constant pressure of 4.6 MPa and a temperature driving force ($\triangle T$) of 4.0 °C. Number in the parentheses indicates the experiment number in Table 2.

bed size for the first stage while the calculated rates are more or less the same for the second stage. In our view, this finding has important implications when data are compared to models. When numerical simulations are performed to validate hydrate reservoir models or simply to compare with experimental data, then laboratory data for different sample sizes must be used. This is especially significant when the model under consideration relies on adjustable parameters. Second, it is recommended that when samples of naturally occurring hydrates are obtained for physical testing, then different sample

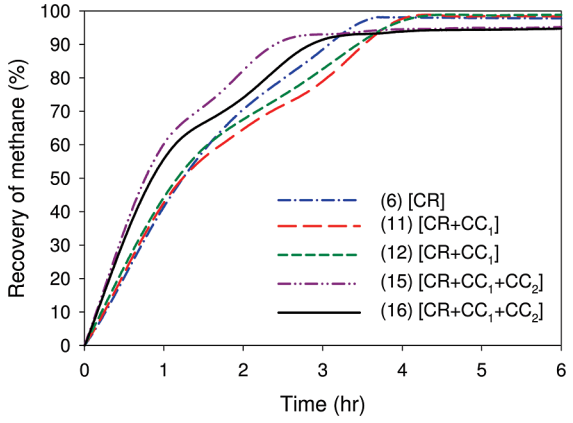

Figure 13. Comparison of percent methane recovery from decomposition experiments for three different silica bed sizes (CR, $CR+CC_1$, $CR+CC_1+CC_2$) studied at a constant pressure of 4.6 MPa and a temperature driving force ($\triangle T$) of 10.0 °C. Number in the parentheses indicates the experiment number in Table 2.

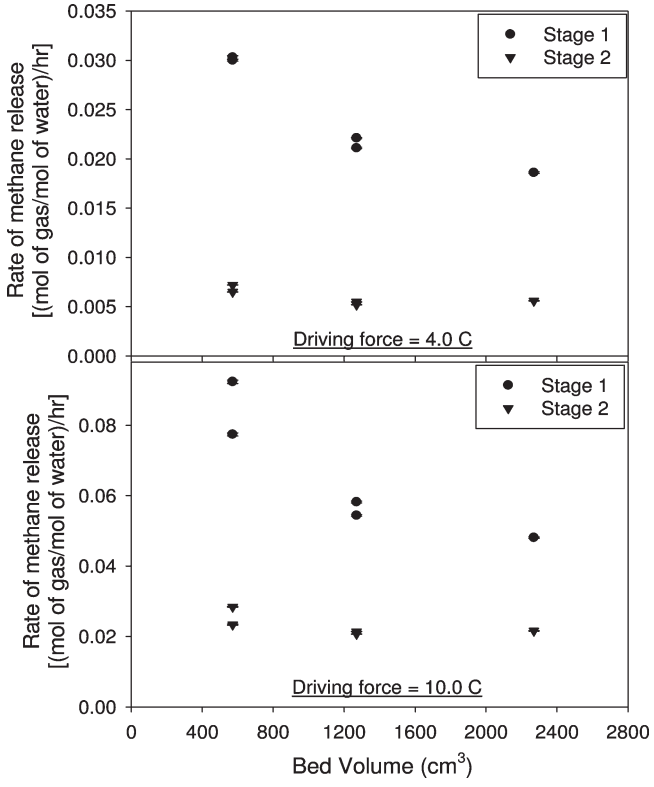

Figure 14. The calculated rates along with the standard errors plotted against the volume of the bed for all the decomposition experiments carried out at a driving force of 4.0 °C (Experiments 5, 9, 10, 13, and 14) and 10 °C (Experiments 6, 11, 12, 15, and 16).

sizes should be obtained for use in hydrate dissociation experiments where the rate of gas release is measured.

4. Conclusions

A new apparatus was set up to study methane hydrate formation and decomposition behavior in the interstitial space of a bed of silica sand particles. The unique feature of this apparatus is the ability to do experiments with three bed sizes. This was achieved by installing one and two copper cylinders in the crystallizer, thereby narrowing the size of the bed with the height of bed kept constant at 7.0 cm. Decomposition of

hydrate by thermal stimulation was carried out for the recovery of the methane from the decomposing hydrate. Recoveries in the range of 95−99% were achieved. The recovery was also found to be faster with a driving force of 10.0 °C compared to that at 4.0 °C, as expected. The results from all experiments indicated that hydrate dissociation occurred in two stages (a faster methane recovery rate was followed by a slower one). Moreover, the rate of methane release (recovery) per mol of water was found to depend on the bed size for the first stage of hydrate dissociation. The implications of the findings on the use of laboratory data and sampling of natural gas hydrates in the earth were discussed.

Nomenclature

n_T = total number of moles
n_H = moles of the gas in hydrate + water phase of Crystallizer
n_G = moles of gas in gas phase of Crystallizer
n_R = moles of gas in Reservoir
V_G = volume of gas phase in Crystallizer
V_R = volume of Reservoir
z = compressibility factor
$(\Delta n_{H,\downarrow})_{t_{end}}$ = number of moles consumed for hydrate formation at the end of a formation experiment.
$(\Delta n_{H,\uparrow})_t$ = number of moles released from hydrates during hydrate decomposition at any given time

Acknowledgment. The financial support from the Natural Sciences and Engineering Research Council of Canada (NSERC) and Natural Resources Canada (NRCan) is greatly appreciated. Dr. Nam would like to thank the Korean Government (MOEHRD) for the Korea Research Foundation Grant (KRF-2006-611-D00006).